Sensors & Actuators: B. Chemical 326 (2021) 128931

Contents lists available at ScienceDirect

Sensors and Actuators: B. Chemical

journal homepage: www.elsevier.com/locate/snb

DWTLSTM for electronic nose signal processing in beef quality monitoring

Dedy Rahman Wijaya [a,*], Riyanarto Sarno [b,1], Enny Zulaika [c,1]

[a] School of Applied Science, Telkom University, Bandung, Indonesia
[b] Department of Informatics, Institut Teknologi Sepuluh Nopember, Surabaya, Indonesia
[c] Department of Biology, Institut Teknologi Sepuluh Nopember, Surabaya, Indonesia

ARTICLE INFO

Keywords:
beef quality monitoring
classification
electronic nose
discrete wavelet transform
long short-term memory
regression

ABSTRACT

The smart packaging system is needed to continuously monitor the quality of beef and microbial population for both the meat industries as well as end consumers. Moreover, several feasibility studies of electronic nose (e-nose) for rapid beef quality assessment are also conducted in recent years. The characteristics of e-nose are fast, cheap, and easy to use make it suitable and scalable for beef quality monitoring applications. It is also potential to be integrated with consumer electronics such as refrigerator and meat chiller. However, the inevitable challenge is how to handle time-series data that is contaminated with noise. In this paper, discrete wavelet transform and long short-term memory (DWTLSTM) is proposed to overcome the e-nose signal contaminated with noise in monitoring beef quality. In beef quality classification task, our proposed has a favorable performance with 94.83% of average accuracy and 85.05% of average F-measure. Moreover, it presents a satisfactory performance in the prediction of microbial population (RMSE = 0.0515 and $R^2 = 0.9712$). These results indicate that the DWTLSTM outperforms conventional methods such as k-nearest neighbor (k-NN), linear discriminant analysis (LDA), support vector machine/support vector regression (SVM/SVR), multilayer perceptron (MLP), and even standard long-short term memory (LSTM).

1. Introduction

During 1961-2011, the demand for animal-based protein (ABP) tends to rise from 23.1 kg/person/year to 42.20 kg/person/year [1]. Moreover, Food and Agriculture Organization (FAO) makes a prediction that beef has a high demand and still becomes one of the main sources of ABP until 2050. Total consumption will increase both in developed countries and developing countries according to this report [2]. These reports show that beef is still a popular food ingredient in the world. Unfortunately, beef is one of the most perishable foodstuffs if it is not handled properly. This is an ideal medium for microbial growth which causes a rapid deterioration in quality due to the breakdown of nutrients present in meat. The beef quality degradation is indicated by changes in texture, color, and odor. The consumption of infected meat products causes various health risks for a human being. Bovine tuberculosis, anthrax, salmonellosis, listeriosis, brucellosis, taeniasis or trichinosis are examples of diseases caused by consumption of infected meat [3]. European Food Safety Authority has been reported that more than 15% of the population in Europe suffers from foodborne diseases. In the USA, about 76 million foodborne illness cases occur each year. Economic losses caused by diseases of major pathogens are estimated at more than $ 35 billion in medical costs and lost productivities every year in the US [4]. Several mechanisms have been introduced for assessing meat quality including sensory panel, total volatile basic nitrogen, total count of bacteria, and gas chromatography. However, most of these methods are only suitable for laboratory scope, need special expertise, time-consuming, laborious, and high-cost [5]. On the other hand, meat industries need a smart packaging system to monitor meat quality and shelf life to minimize spoilage and wastage [6]. Moreover, the low-cost and rapid meat assessment system is appropriate to the end consumers to avoid health risks. In recent years, e-nose is utilized for meat quality classification. Initially, e-nose was applied to differentiate two classes of beef (fresh and spoiled) with excellent classification accuracy (>96%) [7–11]. Afterward, three sensory classes were used to classify beef sample into fresh, semi-fresh, spoiled using e-nose [12–14]. These existing studies demonstrate the ability of e-nose to recognize meat quality. Moreover, e-nose has advantages as follows: relatively fast, cheap, and portable. Thus, it is suitable for online monitoring and analysis [15]. In the case of meat quality monitoring, the e-nose signal is a kind of time-series data that describes the changes in the quality of

* Corresponding author at: Jalan Telekomunikasi, Terusan Buah Batu, Bandung City, West Java, 40257, Indonesia.
E-mail addresses: dedyrw@tass.telkomuniversity.ac.id (D.R. Wijaya), riyanarto@if.its.ac.id (R. Sarno), enny@bio.its.ac.id (E. Zulaika).
[1] Jalan Raya ITS, Keputih, Sukolilo, Surabaya City, East Java, Indonesia (60111).

https://doi.org/10.1016/j.snb.2020.128931
Received 22 May 2019; Received in revised form 12 March 2020; Accepted 16 September 2020
Available online 21 September 2020

meat and the microbial populations. Hence, the appropriate method for time-series data analysis is required.

In e-nose community, artificial neural network families have been reported for e-nose signal processing with remarkable performance, for example, neuro-fuzzy [16], learning vector quantization [17], and fuzzy-wavelet neural network [14]. On the other hand, LSTM is a neural network algorithm that is specifically developed for sequential data processing. It has been reported to deal with several interesting applications related to sequence data analysis such as detection of web traffic anomaly [18], remaining useful life estimation [19], monitoring and fault protection [20], natural language processing [21], air quality prediction [22], etc. In recent years, several studies also attempt to compare different LSTM variants to find the best type of LSTM. However, they cannot make firm conclusions about which the best LSTM variant [23,24]. There is also a paper that claims to do the largest study in LSTM. This study compares eight LSTM variants with different architectures to understand the role of each LSTM component [25]. Three datasets were used to represent different tasks such as speech recognition, handwriting recognition, and polyphonic music modeling. The experimental results denote that all of LSTM variants unable to significantly improve the performance of vanilla LSTM as the baseline. In addition, the impact of hyperparameter was analyzed to find out which parameters were most influential. There are three parameters that have a significant impact on LSTM performance including learning rate, hidden layer size, and noisy input. According to the experimental results, this paper also suggests how to find a good learning rate. It is sufficient to do a rough search by starting with a high value and dividing it by ten until no improvements. Furthermore, the large number of nodes in the hidden layer may present better performance. Nevertheless, it increases computation time and affects the speed of network convergence. To deal with noisy inputs, the authors mentioned that a traditional regularizer was used but noise still affects and it also caused an increase in training time. In addition, the results show that the higher noise levels in the data cause more severe performance degradation and higher computational time than data with low noise [25]. This result implies that the standard LSTM is not too resistant to a noisy signal. The ability to model a complex pattern is one of the advantages of deep learning techniques which are not available in shallow learning techniques. Nevertheless, LSTM does not have a specific mechanism to handle noisy inputs which causes significant performance degradation. Several studies have attention to the input quality of LSTM. LSTM framework has been proposed in traffic flow prediction to tackle missing data. The proposed method presents an improvement of the original LSTM to deal with short-period and long-period missing values [26]. Moreover, the quality of input in LSTM networks is improved using dropout layer [27]. In existing studies, discrete wavelet transform (DWT) is utilized to handle noisy data in LSTM networks [28–30]. However, they do not explain how the DWT parameters are determined to perform signal reconstruction. There is a study that combines DWT, convolutional neural network, and LSTM [31]. The comparison of different wavelet decomposition level is provided, but the way to find the most suitable mother wavelet (MWT) is not discussed. Actually, there are two most important parameters for performing DWT including decomposition level and mother wavelet selection [32]. In fact, signal reconstruction must be carried out carefully to ensure that the reconstructed signal does not lose important information.

In reality, the presence of noise cannot be avoided in almost all e-nose applications. For instance, the fluctuation of gas sensor responses has happened on the practical use in aromatherapy [33]. In severe conditions, e-nose signals can contain much noise with more than 20% noise contamination [34,35]. Internal source of noise such as flicker noise dominates the source of noise which is typically caused by gas molecule adsorption and desorption processes on the gas-sensitive layer [36]. Moreover, external sources of noise such as fluctuating in temperature, humidity, and ambient air also play an important role [37,38]. In many e-nose studies, moving average is a common technique for easy and fast implementation of noise filtering technique. For example, it is combined with restricted Boltzmann machine to detect bacterial infection in blood [39], monitoring of livestock farm odors [40], meat and fish freshness assessment [11], odor detection [41,42], saffron classification [43]. In addition, binomial smoothing is utilized to reduce the noise level in beef spoilage classification [7,8]. Compared to moving average and binomial smoothing filter, DWT has abundant mother wavelet families and decomposition levels that imply it can be used to properly reconstruct noisy signals based on various parameter combinations. Moreover, DWT also considers both low-pass and high-pass filters compared to the moving average that only performs low-pass filtering. For interested readers, more complete discussion about e-nose data processing including challenges and existing methods can be seen in [44,45]. Furthermore, in e-nose signal processing, wavelet coefficient has a better performance than other methods to process signals from metal-oxide-based gas sensors based on radial basis function neural network and principal component analysis [46,47]. The wavelet-based noise filtering framework has been reported to improve the performance of conventional machine learning algorithms in beef quality monitoring [48]. In addition, wavelet filters have also been successfully implemented for noise reduction and signal compression produced by conductor polymer sensors [49]. Based on this background, we have several motivations to perform this study as follows:

1 In the existing studies, the sampling process is performed every 3 days interval [7,8], 4-24 hours interval [12,13], 1 to 3 days sampling interval [10] using limited samples of beef cut (beef strip loin [7,8, 10], beef fillet [12–14,50], and lean beef [15,48,51,52]). In contrast, we are motivated to perform long term monitoring to simulate a smart packaging system using e-nose. In addition, we use various types of beef cuts for the sample. We believe that the different protein and lipid content in each type of beef cut can produce different volatiles emitted that influence the signal patterns. Thus, larger and more comprehensive data can be obtained in this study.
2 The process of meat quality monitoring produces time-series datasets. Therefore, the appropriate method for time-series data processing is needed to produce better performance than conventional methods to perform classification and regression tasks.
3 In particular, several challenges must be faced in this case. Firstly, the process of decaying meat produces water vapor which causes changes in humidity. Changes in humidity level lead to fluctuating gas sensor response [37]. Secondly, protein decomposition yields ethanol and sulfur compounds that can cause sensor poisoning [53]. Thirdly, the susceptibility of sensor saturation that is caused by exposure to various gases in a long period. This extreme condition takes place during the process of storing meat so that the noise contamination in the e-nose signal is unavoidable.

According to these motivations, a noise-resistant time-series data processing method for e-nose signal is relevant to be developed. LSTM is a prominent algorithm for sequence data analysis which has been successfully utilized in several fields. However, to the best of our knowledge, there has been no study on the application of LSTM to e-nose signal processing. Therefore, the LSTM research for processing e-nose signals is still considered new and rare in this field. Actually, it is possible to take advantage of LSTM networks to process the multivariate time-series data generated by the sensor array, especially in the application of e-nose for monitoring. Therefore, in this paper, a noise-resistant LSTM called DWTLSTM was proposed to handle the time series data generated by e-nose.

The rest of this paper is organized as follows. The brief explanation of LSTM principle and the proposed method can be seen in section 2. Section 3 discusses the experiment that encompasses experimental setup, dataset, and results. Finally, the conclusion of this study is explained in section 4.

2. Methodology

In this section, the principle of LSTM is briefly explained. Then, the detailed mechanism of our proposed method (DWTLSTM) is also discussed.

2.1. The principle of LSTM Recurrent Neural Network

In recent years, researchers have developed deep learning algorithms. They also reported the successful implementation in many case studies. Basically, there are two main architectures namely feed-forward and recurrent type. The example of feed-forward model is a convolutional neural network (CNN). It is a prominent example of spatial data processing such as analyzing visual imagery. On the other hand, recurrent model concerns on temporal domain. Hence, it is suitable for time series data analysis. Recurrent Neural Network (RNN) is a typical architecture with the ability to process sequential data in the time domain. Unfortunately, the practical applications of standard RNN architecture are quite limited. This problem is caused by the difficulties during training process. The occurrence of vanishing or exploding gradient problems is the main obstacle to train an RNN model. This problem causes decreased sensitivity over time when new inputs overwrite the activation of hidden layer so the network forgets the first input [54]. Eventually, LSTM was introduced by Hochreiter and Schmidhuber to deal with this problem [55]. LSTM is plainly designed to avoid long-term dependency problem. The comparison of the repeating module between standard RNN and LSTM is depicted by Fig. 1. All RNN families have a chain form of repeating neural network modules. Yellow squares and grey circles denote neural network layers and pointwise operations, respectively. Fig. 1(a) indicates that a standard RNN has a very simple structure with a single hyperbolic tangent (tanh) layer. On contrast, LSTM has four layers which interact in a particular mechanism as shown in Fig. 1(b). It consists of three sigmoid layers (σ) and a tanh layer. The main component of LSTM is cell state. LSTM has ability to add or remove information in the cell state that is regulated by "gates". To regulate the cell state, gates are composed out of a sigmoid layer and a pointwise multiplication operation. The output of sigmoid layer is between zero and one that describing how much information should be let through. Zero value indicates a gate is fully closed and vice versa. An LSTM block has three gates to regulate the cell state including forget gate, input gate, and output gate that is shown in Fig. 4.

2.2. DWTLSTM

In this section, the detail explanations of DWTLSTM are discussed. Aforementioned, the performance of LSTM is highly influenced by noisy inputs from gas sensor array. The presence of noise is definitely harmful to LSTM. It because the LSTM block does not have a particular mechanism to handle noisy inputs. In this research, DWTLSTM is developed to build a prediction model for beef quality monitoring. There are two problems that must be solved. Firstly, the multiclass classification task is needed to differentiate a beef sample into four classes. Secondly, the regression task is carried out to estimate the number of microbes in a beef sample. According to these requirements, there are two types of outputs: discrete output for beef classification task and continuous output for microbial population regression task. Fig. 2 shows the schematic structure of the proposed DWTLSTM. Assume that $x = (x^1, x^2, \ldots, x^m)$ is a raw sensor data where m is a number of the gas sensor in the sensor array (we used 11 gas sensors). In this study, we develop two different models for classification and regression. First, a classification model is used to differentiate four sensory classes of beef. Second, a regression model is needed to predict the total viable count (TVC) in a beef sample. Their difference is only in the output layer. In this experiment, k-NN, LDA, MLP, and SVM/SVR used the reconstructed signals based on DWT as inputs to produce the best result for a fair comparison to LSTM and DWTLSTM.

DWT layer performs noise filtering to make sure the quality of signal inputs. In many areas, DWT is a prominent method for non-stationary

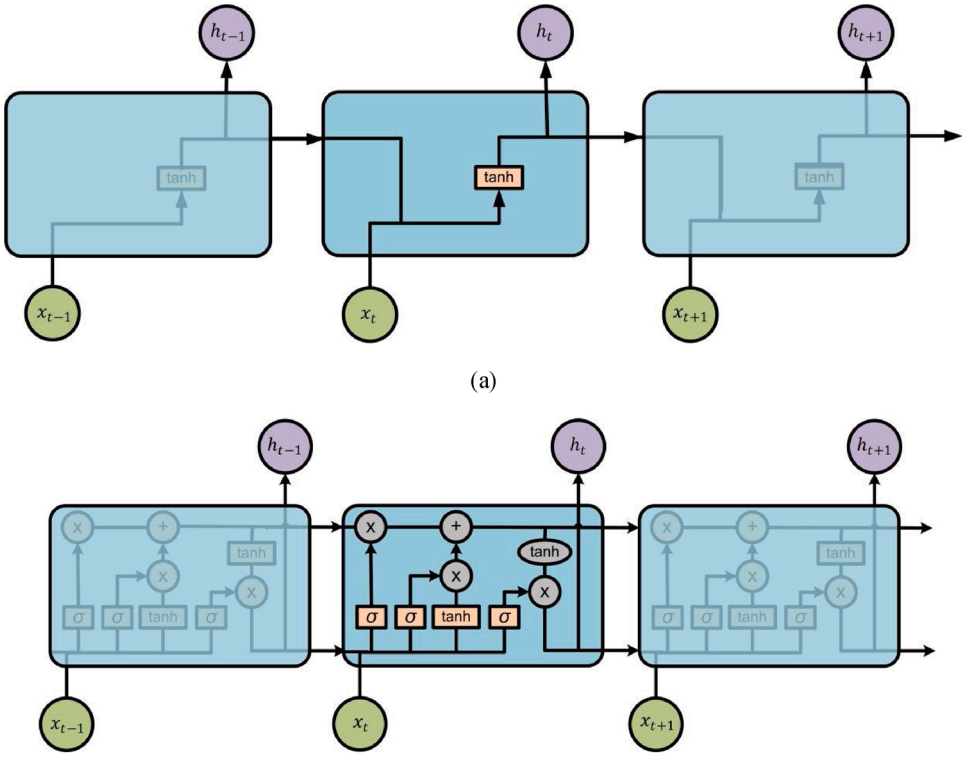

Fig. 1. The comparison of the repeating module: (a) Standard RNN contains a single layer; (b) LSTM contains four interacting layers.

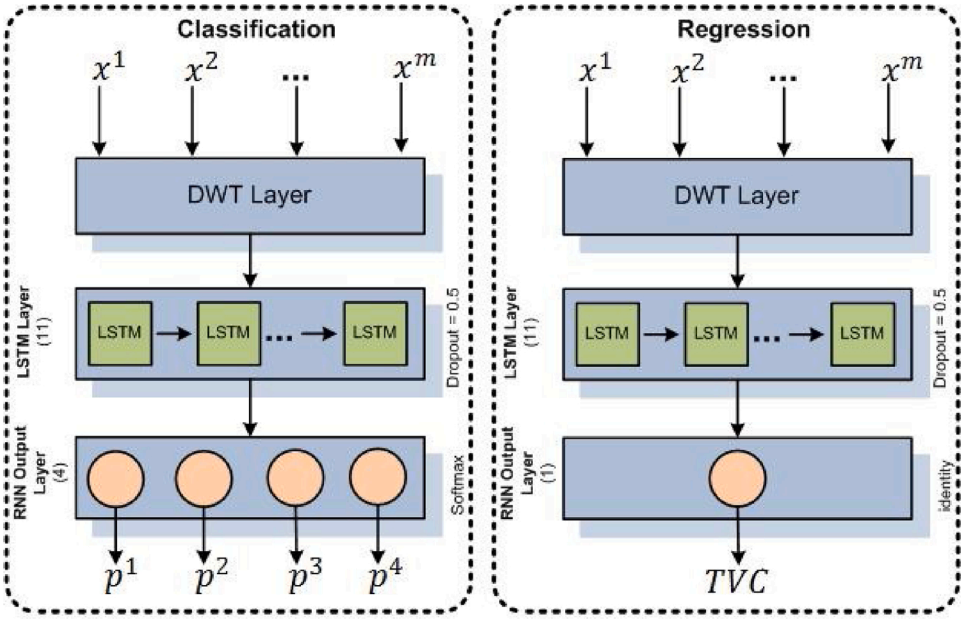

Fig. 2. The structure of proposed DWTLSTM.

signals analysis. It is typically used for signal denoising. The first reference of wavelet transform is about the research of orthogonal systems of functions that led to the development of a set of rectangular basis functions [56]. Performing DWT for given signal ($x(t)$) can be mathematically expressed by

$$dwt(v,w) = \langle x(t), \psi_{v,w}(t) \rangle = \frac{1}{\sqrt{2^v}} \int_{-\infty}^{\infty} x(t)\psi^*\left(\frac{t - w2^v}{2^v}\right)dt \tag{1}$$

where v and w denote wavelet scaling and translation parameter, respectively [56,57]. Then, $\psi^*()$ means the complex conjugation of MWT ($\psi(t)$). Several MWT families can be used according to signal characteristics such as haar, symlet, daubechies, coiflet, biorthogonal, reverse biorthogonal, and meyer wavelet. In DWT implementation, MWT selection is needed to ensure that the reconstructed signal can represent the information content of the original signal. In multilevel wavelet transform, there are two wavelet coefficients namely approximate and detailed coefficient. Hence, the reconstruction of signal $x(t)$ can be satisfied by

$$x(t) = \sum_{v=\infty}^{V} \sum_{w=\infty}^{\infty} d_{v,w}\psi_{v,w}(t) + \sum_{w=\infty}^{\infty} a_{v,w}\phi_{v,w}(t) \tag{2}$$

where a, d and $\varphi(t)$ denote the approximate coefficient, detailed coefficient, and scaling function, respectively. Moreover, the following equation expresses the signal that contaminated with noise:

$$x(t) = y(t) + \rho * n(t) \tag{3}$$

where $x(t)$, $y(t)$, $\rho, n(t)$ imply original (noisy) signal, reconstructed signal, noise level and noise function, respectively. The objective of noise filtering is to suppress the noise level. Commonly, the process of noise filtering contains three main steps as follows [57]:

1 Signal decomposition, determining a decomposition level (V) and a best-suited MWT (ψ);
2 Thresholding, applying a threshold to the detail coefficients for every decomposition level (1 to V);
3 Signal reconstruction, obtaining the reconstructed signal based on an approximate coefficient from level V and the detailed coefficients from level 1 to V.

Nevertheless, the problem of the noise filtering process is how good the capability of DWT to suppress the noise in the reconstructed signal with still keeps the essential information? It really depends on the decomposition level and the selected MWT. The proper signal reconstruction is needed to keep important information contained in the signals. The first question is how to find the right level of wavelet decomposition? A decomposition level that is too low causes not optimum noise filtering process. Conversely, too high a decomposition level causes signal damage due to loss of essential information [32]. Moreover, the highest level of wavelet decomposition not necessarily gives the best result [58]. Hence, the decomposition level should not be carelessly decided. The way to determine the level of decomposition must satisfy the rules [57]:

$$\frac{F_{sample}}{2^{L+1}} \le F_{char} \le \frac{F_{sample}}{2^L} \tag{4}$$

where F_{sample}, F_{char}, L mean sampling frequency, frequency characteristic, and length of the signal, respectively. The second question is how to determine the best-suited MWT? In this experiment, information quality becomes our main consideration to find the best-suited MWT for each signal. A high-quality reconstructed signal means that it can store important information from the original signal. Related to this issue, the determination of best-suited MWT should be based on a measure of the quality of information. In this study, the information quality ratio (IQR) is utilized to determine the most appropriate MWT. The IQR value of the original signal ($x(t)$) and the reconstructed signal ($y(t)$) can be computed by the following equation [32]:

$$IQR(x(t), y(t)) = \frac{\sum_{x\epsilon x(t), y\epsilon y(t)} p(x,y) log_2(p(x)p(y))}{\sum_{x\epsilon x(t), y\epsilon y(t)} p(x,y) log_2(p(x,y)) - 1} \tag{5}$$

$x, y, p(x), p(y), p(x,y)$ show the specific value of the raw signal, the certain value of the denoised signal, the marginal probability function of raw signal, the marginal probability function of denoised signal, and the joint probability function of two signals, respectively. IQR is utilized to compare several MWTs to find the most appropriate MWT. The range of IQR value is between 0 and 1. IQR = 0 indicates that the reconstructed signal completely loses important information from the original signal. In other words, the chosen MWT is not compatible with the original signal. In contrast, IQR = 1 means the selected MWT can perfectly

reconstruct the original signal without losing important information. The most appropriate MWT is determined for each signal produced by the gas sensor. Moreover, this following $m \times n$ matrix shows IQR values of m signals denoised by n different MWTs.

$$\boldsymbol{IQR}_{\boldsymbol{m\times n}} = \begin{bmatrix} IQR_{1,1} & \cdots & \cdots & IQR_{1,n} \\ \cdots & \cdots & \cdots & \cdots \\ \cdots & \cdots & \cdots & \cdots \\ IQR_{m,1} & \cdots & \cdots & IQR_{m,n} \end{bmatrix}$$

Hence, the most appropriate MWTs for m signals can be found by the maximum value of IQR in every row as follows:

$$\begin{bmatrix} IQR^{1}_{best} \\ \vdots \\ IQR^{m}_{best} \end{bmatrix} = \begin{bmatrix} \max(IQR_{1,1} \ldots IQR_{1,n}) \\ \vdots \\ \max(IQR_{m,1} \ldots IQR_{m,n}) \end{bmatrix} \quad (6)$$

Fig. 3 shows the procedure to find the DWT parameters including decomposition level and MWT for each signal. In the first step, the decomposition level is determined because it has a high impact on selected MWT. In addition, an inappropriate level of decomposition leads to not optimal signal reconstruction and signal distortion [32]. According to Eq.(4), the decomposition level can be ascertained. Denoising and compressing for raw signal are performed based on decomposition level and MWT in the second and third steps, respectively. In the fourth step, IQR value between raw and reconstructed signal is calculated. In this study, 38 MWT families were compared including daubechies, symlet, coiflet, biorthogonal, and dmey. Hence, this process is repeated 38 times for each signal to determine the best MWT with the highest IQR value based on Eq.(6) in the fifth step. According to this process, Table 1 shows the parameters in the DWT layer for each sensor/signal. More detail process of DWT parameter comparison can be seen in our previous study [32].

After performing DWT, min-max normalization is used to equalize the scale of the reconstructed signal. We ensure that min-max normalization has been reported for satisfactory performance in supervised and unsupervised learning [59–61]. The signals are fed into the LSTM layer and processed by LSTM blocks. In this experiment, LSTM layer contains 11 LSTM blocks. The detail data flow in an LSTM block is shown in Fig. 4.

LSTM has the ability to add or remove information to the cell state which is regulated by gates. Gates act as a filter that determines the information forwarded or not. They consist of a sigmoid neural network layer and a pointwise multiplication operation. The first step of LSTM is to determine the information which wants to be deleted from the current cell state. This decision is made by a sigmoid layer namely "forget gate layer". In Eqs. (7)–(12), $\boldsymbol{W}, h_{t-1}, h_t, x_t, b$ denotes weight matrix, previous output, current output, current input, and bias, respectively. The forget gate layer can be expressed by the following equation.

$$f_t = \sigma\left(\boldsymbol{W}_f.[h_{t-1}, x_t] + b_f\right) \quad (7)$$

The output value of forget gate layer (f_t) generated by the sigmoid function is between 0 and 1. Using a pointwise multiplication operation, it can be determined whether the previous cell state (C_{t-1}) is kept or not. $f_t = 1$ implies that the cell state is completely kept and vice versa. Furthermore, new information is stored in the cell state. Sigmoid layer namely "input gate layer" decides which value will be updated (i_t). The operation of this layer can be expressed as follows:

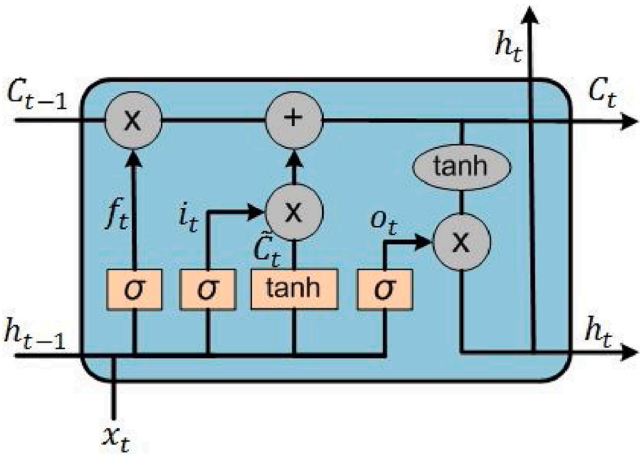

Fig. 4. A detailed schematic of LSTM block.

Table 1
The parameters in DWT layer.

No	Sensor	MWT	Level of decomposition
1	MQ135	bior2.4	11
2	MQ136	bior3.3	11
3	MQ137	bior2.8	10
4	MQ138	db1	10
5	MQ2	db1	11
6	MQ3	bior3.3	10
7	MQ4	db1	10
8	MQ5	sym6	10
9	MQ6	bior2.2	11
10	MQ8	dmey	10
11	MQ9	db1	10

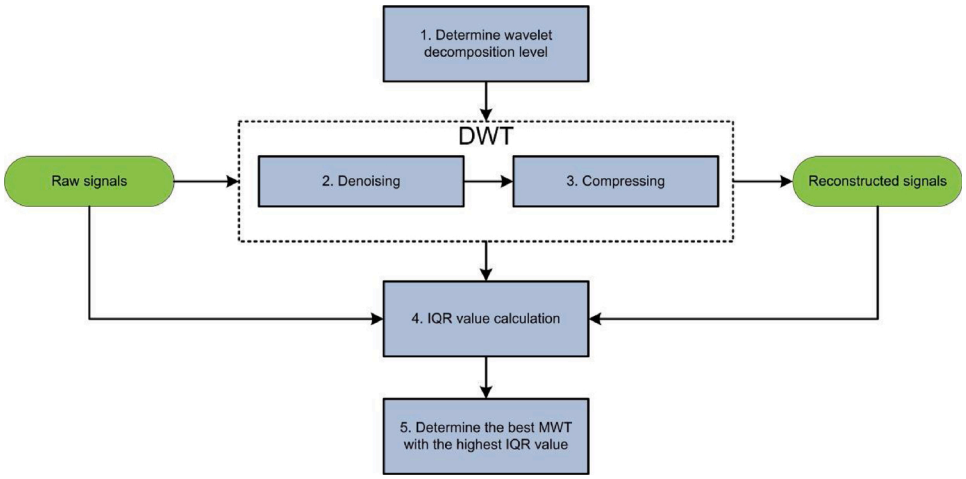

Fig. 3. The procedure to determine wavelet decomposition level and MWT.

$$i_t = \sigma(\boldsymbol{W}_i.[h_{t-1}, x_t] + b_i) \tag{8}$$

Then, a tanh layer produces a vector of new cell state candidate ($\tilde{C}_t$) which is added to the state. The process can be expressed by:

$$\tilde{C}_t = tanh(\boldsymbol{W}_C.[h_{t-1}, x_t] + b_C) \tag{9}$$

The next step is to update the old cell state (C_{t-1}) to the new cell state (C_t). The old state is multiplied by f_t which acts as forget gate. Then, this result is added with $i_t \times \tilde{C}_t$. Hence, the operation of cell state update can be mathematically expressed as follows:

$$C_t = f_t \times C_{t-1} + i_t \times \tilde{C}_t \tag{10}$$

Finally, the output is determined based on the cell state in the filtered version. The sigmoid layer as output gate is used to decide what parts of the cell state to become output value (o_t). Then, the cell state is inputted into the tanh function to convert the value between -1 and 1 then multiplied by the result of the sigmoid layer. This process can be expressed by the following equation.

$$o_t = \sigma(\boldsymbol{W}_o.[h_{t-1}, x_t] + b_o) \tag{11}$$

$$h_t = o_t * tanh(C_t) \tag{12}$$

As illustrated in Fig. 2, the proposed DWTLSTM is divided into two models with the difference only in the output layer. In the classification model, the output layer consists of four nodes with a softmax activation function correspond to the number of beef classes. The outputs of the LSTM layer are flattened into a vector $\boldsymbol{h} = (h_1, h_2, \ldots, h_m)$, where m is the number of LSTM blocks in the last layer. Given input $\boldsymbol{h}$ for total C output neurons correspond to the number of classes, the softmax activation function for multiclass classification can be computed by

$$P(ch) = \underset{c \in C}{\operatorname{argmax}} \left\{ \frac{e^{\boldsymbol{h}^{\mathrm{T}} \boldsymbol{w}_c}}{\sum_{k=1}^{N_c} e^{\boldsymbol{h}^{\mathrm{T}} \boldsymbol{w}_k}} \right\}, \tag{13}$$

where $\boldsymbol{w}$ and $\boldsymbol{h}^{\mathrm{T}}\boldsymbol{w}$ denote the weighting vector and inner product of $\boldsymbol{h}$ and $\boldsymbol{w}$, respectively. Based on Eq.(13), the class of beef can be detected based on the highest probability value.

Algorithm 1. Model Training

Algorithm 1: Model Training

Input: training data, validation data, and testing data for classification (discrete labels) or regression (continuous labels)
Output: the best model for classification or regression

```
1  dTraining ← load(data_training)
2  dValidation ← load(data_validation)
3  dTesting ← load(data_testing)
4
5  NormalizerMinMaxScaler(dTraining, 0, 10)
6  NormalizerMinMaxScaler(dValidation, 0, 10)
7  NormalizerMinMaxScaler(dTesting, 0, 10)
8  MultiLayerNetwork net ← new MultiLayerNetwork(conf)
9  epoch ← 1000
10 for i ← 1 to epoch do
11         net.fit(dTraining)
12         predicted ← net.output(dValidation)
13         evaluation(actual, predicted)
14         if (mode = 'classification') then
15                 current_accuracy ← evaluation.getAccuracy()
16                 current_f1 ← evaluation.getF1()
17                 //Early stopping for classification
18                 if (best_accuracy < current_accuracy and current_f1 > 80) then
19                         best_accuracy ← current_accuracy
20                         //Save the best model for classification
21                         best_net ← net
22                 end if
23         else if (mode = 'regression') then
24                 current_mse ← evaluation.getMSE()
25                 current_r2 ← evaluation.getR2()
26                 //Early stopping for regression
27                 if (best_mse > current_mse and current_r2 > 0.8) then
28                         best_mse ← current_mse
29                         //Save the best model for regression
30                         best_net ← net
31                 end if
32         end if
33 end for
```

shows the training process for classification and regression. The performance of classification tasks is investigated based on accuracy and F-measure. For regression tasks, mean squared error (MSE) and R-squared (R^2) are utilized to measure prediction model performance. In this experiment, the training was performed during 1000 epoch. In every epoch, the model was evaluated to find the best model using these metrics. For the classification model training, the current model will be replaced by a new model if the new model accuracy is higher than the current model. Moreover, this pre-requisite of model updating is fulfilled if F-measure value more than 80%. This threshold is given to guarantee that four beef classes can be predicted by the model. For instance, F-measure value is 75% susceptible that the model can only predict three classes because of the low recall value. Therefore, ensuring the F-measure value above 75% is necessary. Furthermore, in the regression model training, the determination of the best model is based on the MSE value. The new model with lower MSE value is used to replace the current model. R^2 is utilized as a threshold to determine

whether the current model will be updated or not. In this experiment, the new model is considered if R^2>0.8. According to our experience, if the R^2 value is lower than 0.8, the model cannot present a favorable performance. For hyperparameter optimization, a grid search was used. The best learning rate was searched from [10^{-1}, 10^{-2}, 10^{-3}, 10^{-4}, 10^{-5}]. Regularization and dropout methods were used to avoid overfitting. In this experiment, the l2 regularization value was searched from [10^{-3}, 10^{-4}, 10^{-5}, 10^{-6}] and the dropout rate was 0.5.

3. Experiments

In this section, the experimental setup is explained including materials, datasets, and performance measures. The results are discussed including classification of beef quality and regression to predict TVC value of the microbial population.

3.1. Experimental setup and dataset

In this experiment, the self-developed e-nose system is utilized to monitor a beef sample. The e-nose device is composed of the gas sensor array, microcontroller, and WiFi-shield. Metal-oxide semiconductor (MOS) gas sensors are assembled to Arduino microcontroller. In this experiment, MQ gas sensors from Zhengzhou Winsen Electronics Technology Co., Ltd. were used. Table 2 denotes MOS gas sensors used in e-nose. MOS gas sensor type is chosen because it has advantages of good sensitivity, low-cost, and short response time [62]. This gas sensor has been reported for successfully used to various applications including detection of aging beer [63], bacteria detection in the wound [64], halal authentication [65], blood glucose level detection [66], and quality of pecan evaluation [67]. In addition, MOS gas sensor is a type of heat sensor that is not too sensitive to humidity compared to cold sensor types [68]. Therefore, it is more appropriate to monitor meat quality due to fluctuating humidity in the sample chamber. The gas sensor selectivity is determined based on gases produced by the protein degradation process including carbon dioxide, hydrogen sulfide, ammonia, methane [69]. Aldehyde, ketone, hydrogen, and alcohol compounds are also noticed during beef spoilage from carbohydrate degradation [68,70].

The gas sensor resistance value (R_s) is calculated as a response based on the analog to digital (ADC) value as given as follows:

$$R_s = \frac{V_C - V_{RL}}{V_{RL}} \times RL \tag{14}$$

where

$$V_{RL} = \frac{V_C \times ADC}{1023} \tag{15}$$

V_C, V_{RL}, RL, ADC denote standard voltage of microcontroller (5 V), current sensor voltage, sensor load resistance (based on ohm meter), and ADC value, respectively. R_s value represents the response of resistive sensor type (MOS gas sensor) that is utilized in this experiment. For faster gas detection, the sample space is placed at the bottom of the sensor array. In this experiment, we attempt to control the temperature in order to make the gas sensor response more stable. Hence, e-nose sensor box is placed into the temperature control box. In the temperature control box, three Peltier cooling modules were utilized as cooling elements. Moreover, this temperature was controlled by a thermostat. The temperature cooling box is made of Styrofoam material. The sensor box container is made of transparent acrylic material. Fig. 5 shows the detailed scenario used in this experiment. Wireless access point is used to connect all devices in this experiment including e-nose sensor box, raspberry pi, and computer. Firstly, the encoded responses of gas sensor array are sent to raspberry pi through wireless network. Secondly, signal from e-nose sensor box is received and decoded by middleware that is installed in raspberry pi. Then, the decoded signal is stored in MySQL database. Thirdly, the collected signals are retrieved to computer for signal pre-processing as well as classification and regression by machine learning algorithms.

In this experiment, the temperature is kept at ±31 °C which is depicted in Fig. 6 (a). Fluctuations only occur early in the experiment because the cooling module takes time to stabilize the temperature. Conversely, humidity remains unstable as shown in Fig. 6 (b).

Furthermore, the sample of raw signals contaminated with noise is shown in Fig. 7. It indicates that the noise still exists even though the temperature has been controlled. Therefore, denoising is still needed to reduce the noise level in the raw signals. Fig. 7 also exhibits an example of signal reconstruction using DWT. The left and right figures denote raw and reconstructed signals, respectively. Each color indicates different responses of gas sensors in sensor array that are represented by sensor resistance (ohm). Moreover, each gas sensor produces noisy signals that have different magnitudes. Hence, proper noise filtering is needed to reconstruct raw signals.

In this experiment, twelve types of beef were observed including top sirloin, round (shank), tenderloin, striploin (shortloin), flap meat (flank), clod/chuck, brisket, rib eye, skirt meat (plate), shin, inside/outside, and fat. Each piece of beef contains a different protein and lipid composition. In aerobic conditions, some gases are produced as results of protein decomposition including carbon dioxide, hydrogen sulfide, ammonia, and methane. For lipid decomposition, the neutral fat is hydrolyzed to produce unsaturated fatty acid then the oxidation of this fatty acid can generate aldehydes and ketones [69]. Hence, there is important to use the various beef cuts because the possibility of different sensor responses corresponds to different beef cuts. In this experiment, we used 125 grams for each piece of meat. Using wireless network, the sensor resistance values generated by sensor box are sent to raspberry pi every minute. The data were continuously recorded during 2220 minutes for each experiment cycle that is sufficient to record beef quality from fresh until spoiled. After one experimental cycle completes, the sensor box and the temperature control box were flushed using a high-speed fan to neutralize the odor. After that, they were rested for 3-6 hours to neutralize the remaining odor from the previous experiment. This procedure is repeated for all cuts of beef. In one experiment, we got 2220 measurement points from one piece of beef. Thus, we have a total of 26640 measurement points from twelve datasets corresponding to twelve pieces of beef. To shorten the mention, each dataset that is generated from each beef cut is denoted by DS1 to DS12. As mentioned above, this experiment records the data generated by the e-nose which is continuously sent every minute to the server. Therefore, e-nose can record the process of decaying beef at each stage more precisely. Based on this scenario, this experiment can obtain larger and more comprehensive data than existing studies. In this experiment, the beef quality standard refers to meat standards published by the Agricultural and Resource Management Council of Australia and New Zealand [71]. Meat quality is differentiated into four sensory classes in conjunction with the total viable count (TVC) that is demonstrated in Table 3.

Therefore, the ground truth data refers to the total number of bac-

Table 2
List of used gas sensors

Gas sensor	Selectivity
MQ135	Ammonia, carbon dioxide, alcohol, benzene, smoke, NOx
MQ136	Hydrogen sulfide
MQ137	Ammonia
MQ138	Aldehydes, alcohols, ketones
MQ2	Methane, alcohol, liquefied petroleum gas (LPG), hydrogen, smoke, propane, i-butane
MQ3	Alcohol, benzine, methane, hexane, LPG, carbon monoxide
MQ4	Methane
MQ5	Hydrogen, LPG, methane, carbon monoxide, alcohol
MQ6	Propane, LPG, iso-butane
MQ8	Hydrogen
MQ9	Methane, carbon monoxide, and propane

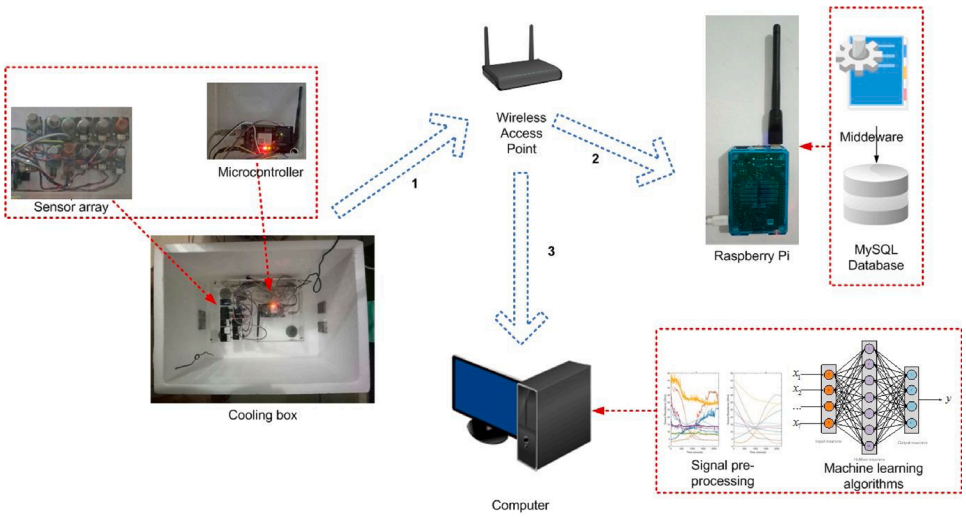

Fig. 5. The scenario of experiment.

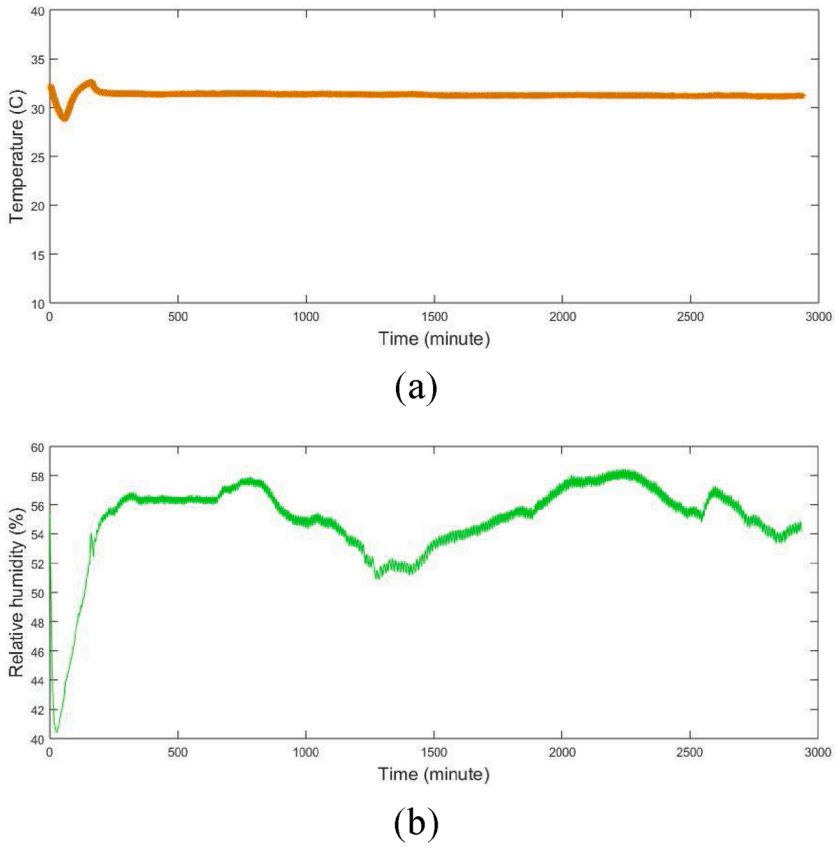

Fig. 6. Example of ambient conditions: (a) temperature; (b) humidity.

teria as the main standard for beef quality. In this experiment, similar numbers of beef samples are tested to quantify the microbial population. The types of beef are also similar to the beef used in the experiment to acquire e-nose signals. Our consideration is the different protein and lipid content in each type of beef cut can produce different volatiles emitted that influence the signal patterns. In this experiment, a spectrophotometer is employed to quantify optical density (1000x dilution). To calculate the microbial population in beef samples, the hemocytometer was utilized. As a rule of thumb, the combination of classical and two-hour method is utilized [72]. Hence, the microbial population is measured every hour for 37 hours for more precise results. Furthermore, this ground truth data is used to label the data contained in the dataset. These datasets are randomly divided for training (50%), validation (25%) and testing data (25%). In this experiment, our proposed method was compared with several machine learning algorithms such as k-NN, LDA, SVM/SVR, MLP, and original LSTM. DWT is also performed to obtain the best result of k-NN, LDA, MLP, and SVM/SVR. For k-NN, Euclidean distance is utilized as the distance metric and the best of k value is searched from [3,5,7,9,11]. In MLP, the neural network architecture is similar to LSTM with a single hidden layer. Hyperbolic tangent is utilized for activation function. Radial basis function kernel is used in SVM/SVR and the best regularization parameter (C) is determined from

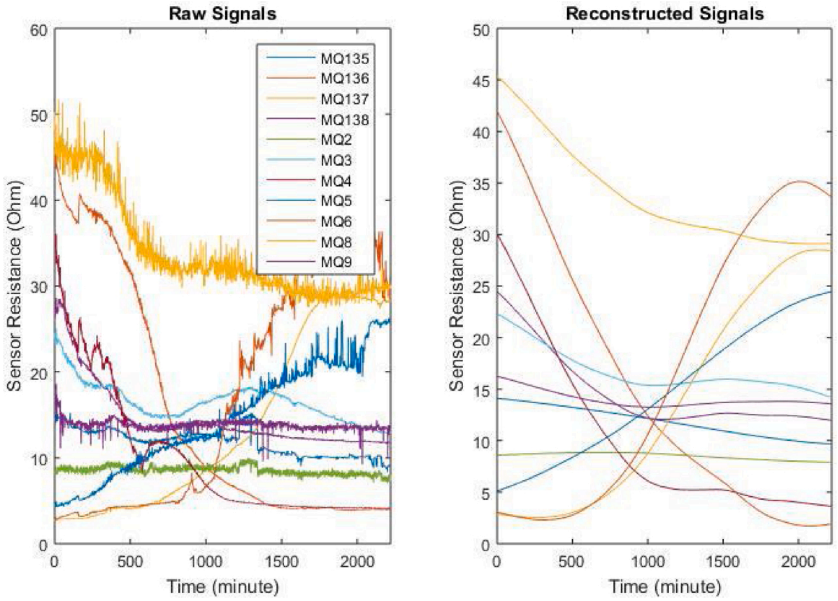

Fig. 7. The example of raw signals (left) and reconstructed signals (right).

Table 3
The beef quality standard,

Class	TVC ($\log_{10}$ cfu/g)
Excellent	< 3
Good	3-4
Acceptable	4-5
Spoiled	>5

*cfu/g: colony forming unit of bacteria in a gram of meat.

[0.001, 0.01, 0.1, 1, 10]. In addition, the experiments are performed on a personal computer with Intel(R) Core(TM) i3-4150 CPU @3.50 GHz (4 CPUs), 4GB RAM, and Windows 7 Professional 64-bit operating system. DWT, k-NN, LDA, and SVM is computed using MATLAB 2015a. LIBSVM is utilized as library for SVM/SVR [73]. MLP, LSTM and DWTLSTM are implemented using Deeplearning4j (DL4J) framework [74]. Classification accuracy and F-measure are used to measure the performance in classification tasks. The classification accuracy and F-measure can be calculated as follows:

$$accuracy = \frac{tp + tn}{tp + tn + fp + fn} \times 100\% \tag{16}$$

and

$$F - measure = 2 \times \frac{precision \times recall}{precision + recall} \times 100\% \tag{17}$$

where

$$precision = \frac{tp}{tp + fp} \times 100\% \tag{18}$$

$$recall = \frac{tp}{tp + fn} \times 100\% \tag{19}$$

tp, fp, tn, fn indicate true positive, false positive, true negative, and false negative, respectively. In the regression task, mean squared error (MSE) and r-squared (R^2) are used for performance metrics. They can mathematically be expressed by

$$MSE(a,p) = \frac{1}{L}\sum_{i=1}^{L}(a_i - p_i)^2 \tag{20}$$

and

$$R^2(a,p) = 1 - \frac{\sum_{i=1}^{L}(a_i - p_i)^2}{\sum_{i=1}^{L}(a_i - \overline{a})^2} \tag{21}$$

where a, p, L denote actual value, predicted value, and total samples, respectively.

3.2. Results and discussion

In this section, the results are discussed including the performance of the proposed method on beef quality classification and prediction of the microbial population.

3.2.1. Beef quality classification

In order to verify the advantages of the proposed method, we compare the performance of DWTLSTM and LSTM not only based on the final results but also during the training process. Fig. 8 shows the accuracy and F-measure during 1000 epoch in the training process based on validation data. Magenta and green marks denote the performance of DWTLSTM and LSTM, respectively. In this study, stochastic gradient descent (SGD) is utilized for neural network learning. In SGD, a few samples are randomly selected for each iteration to find the best parameters. Hence, the path that is taken by SGD is usually no smoother (fluctuating) compared by a typical gradient descent algorithm. According to this random method, when the neural network gets the best performance during training cannot be predicted. However, SGD can significantly reduce training time and computational overhead. During the training process, LSTM has difficulty in modeling signals that are contaminated by noise. This can be proven by the instability of the accuracy value and the F-measure value during the training process. This result indicates that a standard LSTM is more difficult to converge when consuming noisy data. On the other hand, DWTLSTM shows better performance after the 200th epoch which is related to the effect of the SGD mechanism. It produces a more stable performance and leading to a convergence solution compared with standard LSTM. Therefore, DWTLSTM has a better guarantee to find the best model than standard LSTM.

Table 4 denotes the comparison of classification accuracy produced

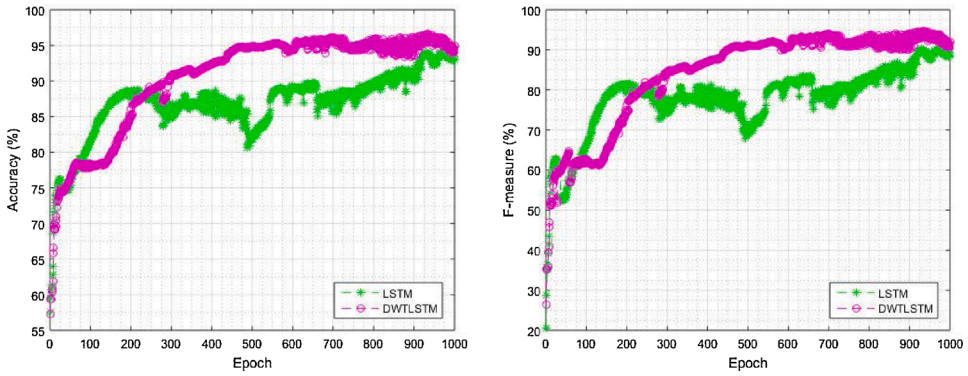

Fig. 8. Accuracy and F-measure values during the training process (magenta: DWTLSTM, green: LSTM): (a) Accuracy; (b) F-measure.

Table 4
The comparison of accuracy (%)

	DS1	DS2	DS3	DS4	DS5	DS6	DS7	DS8	DS9	DS10	DS11	DS12	Average
k-NN	82.70	87.39	76.40	81.62	75.50	83.96	81.26	61.44	79.28	75.68	77.30	70.27	77.73
LDA	84.86	74.95	91.71	79.46	82.88	85.05	74.59	63.24	63.60	72.97	77.48	70.99	76.82
SVM	92.79	88.29	84.14	89.19	81.26	94.95	87.93	72.97	81.62	84.50	80.00	80.90	84.88
MLP	82.16	72.97	20.90	75.86	59.46	77.30	72.97	59.46	72.97	13.51	55.86	10.81	56.19
LSTM	86.67	95.68	93.33	93.33	97.12	96.94	93.69	92.97	89.91	97.66	38.20	46.13	85.14
DWTLSTM	96.04	94.05	94.95	92.79	96.94	93.33	96.94	96.40	97.30	86.31	95.50	97.48	**94.83**

Table 5
The comparison of F-measure (%).

	DS1	DS2	DS3	DS4	DS5	DS6	DS7	DS8	DS9	DS10	DS11	DS12	Average
k-NN	37.66	65.00	22.49	48.48	17.07	44.72	50.00	3.60	34.29	21.97	27.59	-	33.90
LDA	36.36	13.66	65.67	38.71	43.79	45.03	11.32	6.42	-	-	28.57	4.73	29.43
SVM	70.59	73.47	42.11	73.91	32.47	83.53	72.87	-	57.85	39.44	44.22	51.82	58.39
MLP	-	-	-	-	-	-	-	-	-	-	-	-	-
LSTM	61.86	85.88	81.41	81.41	91.67	90.81	78.53	77.71	64.56	93.26	16.55	3.24	68.91
DWTLSTM	84.51	79.50	84.95	78.49	91.37	81.03	90.17	90.00	91.89	70.31	87.05	91.36	**85.05**

by several algorithms. For a fair comparison, DWT (noise filtering) is also performed to obtain the best result of k-NN, LDA, MLP, and SVM. According to the results, MLP gets the lowest average accuracy (56.19%). It implies that the conventional neural network cannot properly model the time series data from e-nose. Moreover, k-NN and LDA get almost similar accuracy with 77.73% and 76.82%, respectively. The best result of the conventional algorithm is obtained by SVM with 84.88%. Standard LSTM gets slightly higher accuracy than SVM with 85.14%. On the other hand, DWTLSTM surpasses other algorithms with 94.83% of classification accuracy. In addition, Table 5 shows more detail performance measure based on F-measure. k-NN and LDA produce the lowest average F-measure with 33.90% and 29.43%, respectively. F-measure score of k-NN is very low, especially in DS8 with 3.60%. Furthermore, in DS12, F-measure score is no available because it can only detect two classes ("excellent" and "spoiled"). Using LDA, the beef quality classification also cannot give satisfactory results because it has no capability to predict all classes in DS9 and DS10. LDA cannot predict "acceptable" class in DS9 and DS10. Moreover, SVM got 58.39% of average F-measure. Unfortunately, it cannot detect "good" and "acceptable" classes in DS8, so F-measure score cannot be calculated. The worst performance is produced by MLP that it cannot completely detect all classes in all datasets. This limitation of k-NN, LDA, and MLP

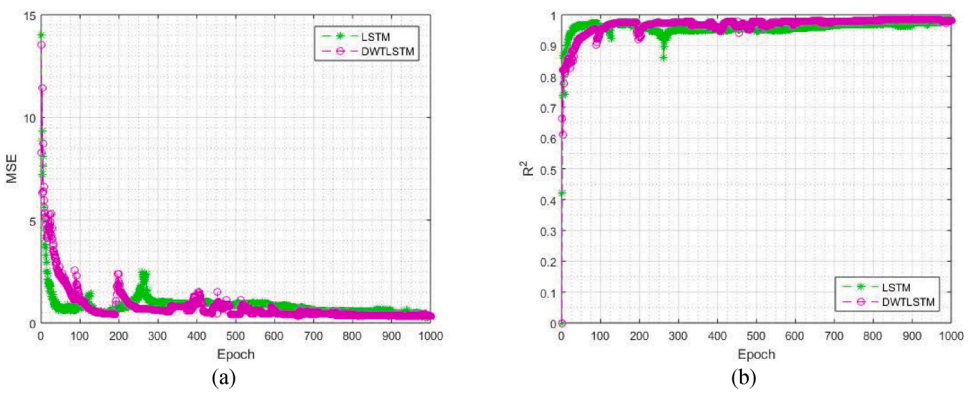

Fig. 9. MSE and R^2 values during the training process (magenta: DWTLSTM, green: LSTM): (a) MSE; (b) R^2.

becomes a serious problem because the detection of gradual changes in beef quality is necessary for the meat industry. The results indicate that k-NN, LDA, MLP, and SVM cannot provide satisfactory performance. Hence, according to our investigation, these conventional methods cannot give a guarantee to completely detect all classes in beef quality classification. On the other hand, LSTM is able to detect four classes of beef in all datasets even though it gets a very low F-measure score in DS12 (3.24%). Unfortunately, this average F-measure score is only 68.91%. The F-measure value that lowers than 75% is susceptible to unable to classify four classes of beef. Moreover, DWTLSTM gets the highest F-measure with 85.05%. The results indicate that DWTLSTM is able to distinguish four classes of beef. All of F-measure scores are higher than 75% except in DS10. The overall results indicate that DWTLSTM has superior performance compared to conventional methods such as k-NN, LDA, MLP, SVM and even standard LSTM in the classification task.

3.2.2. *Prediction of microbial population*

Actually, the regression task to predict the microbial population is more complicated than the classification task. This is because the numeric value of TVC implies the infinite possibilities of class label. Fig. 9 shows MSE and R^2 during the training process based on validation data. Although both fluctuate until 600th epoch, DWTLSTM has more stable MSE values which are almost always lower than LSTM. Likewise with the value of R^2, DWTLSTM is always better than LSTM. These results imply that DWTLSTM is easier to learn the training data than standard LSTM. In this experiment, the performance of DWTLSTM is also compared with k-NN, LDA, SVR, MLP, and standard LSTM for regression task.

For visual observation, the plot of prediction results is depicted in Fig. 10. This figure shows the performance comparison of our proposed method and other algorithms. Black, blue, and red lines denote actual, prediction, and prediction values with error more than 0.5 $\log_{10}$ cfu/g, respectively. Fig. 10a and b show that the performance of k-NN and LDA act as linear regressors. They show that linear regressors produce unstable and rough predictions in all datasets. In several observations, the prediction value equals with actual value. However, the prediction yields a high error in many other observations which are shown by red marks. These results imply that a linear regressor is not suitable for time series e-nose data. Moreover, the performance of SVR is shown in Fig. 10c. SVR with RBF kernel generates finer prediction patterns than linear regressors. Unfortunately, there are still many mistakes, especially in the middle of the observations that the majority of them related

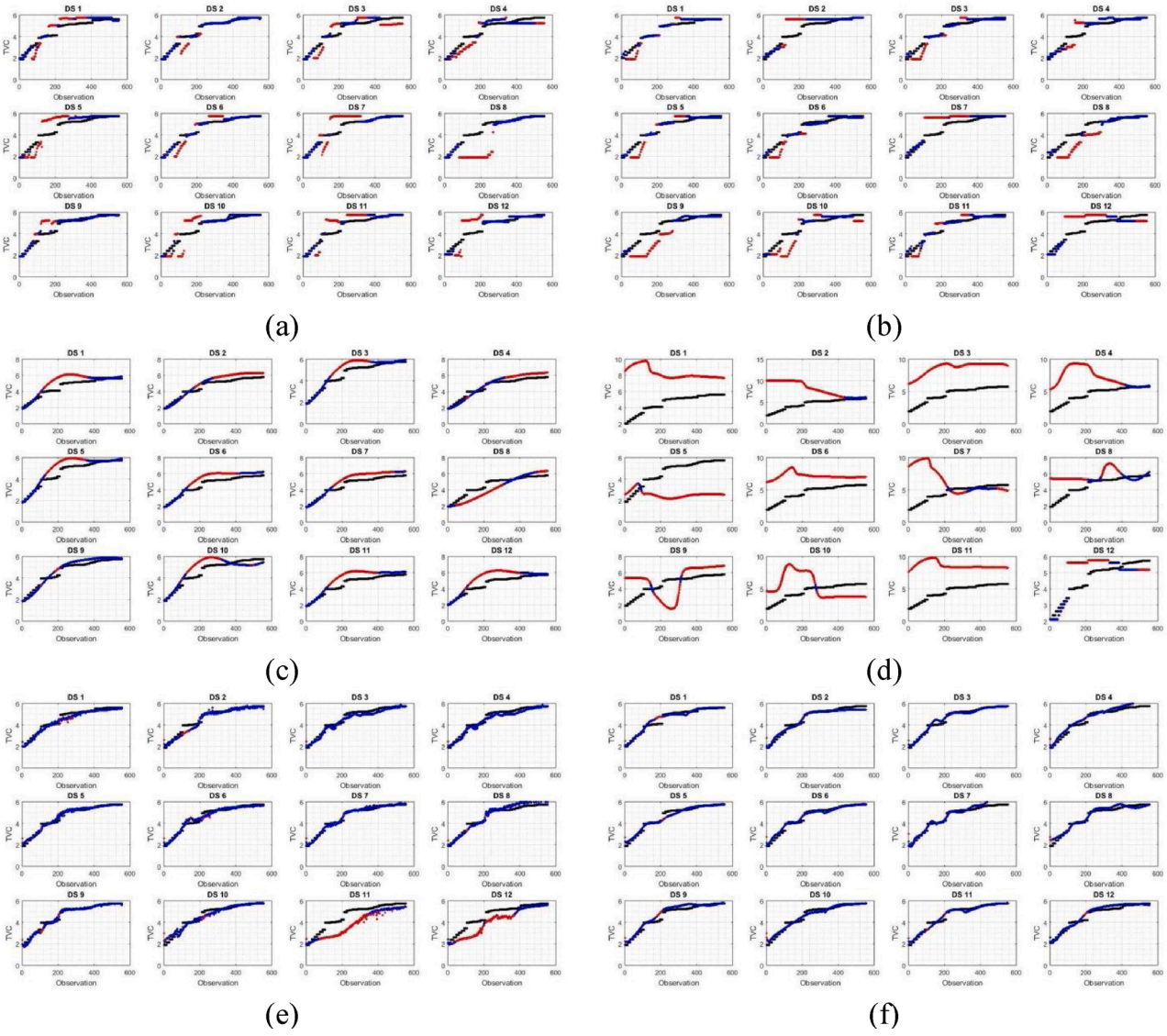

Fig. 10. Plot of regression results (black: actual, blue: prediction, red: prediction with error $\geq$ 0.5 $\log_{10}$ cfu/g): (a) k-NN; (b) LDA; (c) SVR; (d) MLP; (e) LSTM; (f) DWTLSTM.

Table 6
The comparison of MSE.

	DS1	DS2	DS3	DS4	DS5	DS6	DS7	DS8	DS9	DS10	DS11	DS12	Average
k-NN	0.2613	0.1295	0.3179	0.2608	0.4773	0.1791	0.4655	1.9383	0.2114	0.5176	0.3357	0.4832	0.4648
LDA	0.1365	0.4679	0.1815	0.2583	0.2459	0.1997	0.5993	0.6327	0.8324	0.5721	0.1662	0.7222	0.4179
SVR	0.4974	0.2530	0.2595	0.1816	0.3072	0.4139	0.3267	0.5334	0.0906	0.3555	0.5246	0.6815	0.3687
MLP	16.2186	19.0641	16.7277	10.3838	5.9977	7.7480	11.7963	2.2918	3.9753	6.9601	17.7663	8.7729	10.6419
LSTM	0.0513	0.0547	0.0512	0.0512	0.0200	0.0411	0.0203	0.0779	0.0280	0.0610	0.8234	0.4855	0.1471
DWTLSTM	0.0486	0.0411	0.0301	0.0750	0.0419	0.0301	0.0923	0.0500	0.0733	0.0412	0.0339	0.0601	**0.0515**

Table 7
The comparison of R^2.

	DS1	DS2	DS3	DS4	DS5	DS6	DS7	DS8	DS9	DS10	DS11	DS12	Average
k-NN	0.9010	0.9213	0.8066	0.8715	0.8145	0.9165	0.7647	0.5776	0.8850	0.7464	0.8495	0.7142	0.8141
LDA	0.9420	0.7755	0.9179	0.8529	0.8985	0.9167	0.7823	0.8014	0.7895	0.8045	0.8999	0.5711	0.8293
SVR	0.8494	0.9784	0.9240	0.9751	0.9006	0.9462	0.9699	0.8561	0.9745	0.7793	0.9129	0.8431	0.9091
MLP	0.6703	0.7780	0.8402	0.0965	0.3405	0.0014	0.8126	0.1091	0.0320	0.1435	0.1600	0.9871	0.4143
LSTM	0.9716	0.9687	0.9791	0.9791	0.9851	0.9683	0.9876	0.9803	0.9837	0.9538	0.8286	0.9130	0.9582
DWTLSTM	0.9584	0.9746	0.9778	0.9748	0.9699	0.9865	0.9670	0.9666	0.9694	0.9707	0.9740	0.9649	**0.9712**

to "good" and "acceptable" classes. We also used MLP with hyperbolic tangent activation function as a non-linear regressor. However, it still cannot present favorable performance as shown in Fig. 10d. Prediction values highly deviate from the actual values, which means that conventional neural network architecture cannot produce satisfactory performance. Hence, a special type of neural network architecture must be developed. Fig. 10e shows the pattern of prediction of LSTM neural network. The result shows that LSTM has better performance than k-NN, LDA, SVR, and MLP even without noise filtering. However, the performance on several datasets is still unfavorable. It is indicated by many red marks in DS11 and DS12. On the other hand, DWTLSTM shows the performance improvement of LSTM that is depicted in Fig. 10f. It generates a smoother prediction on all datasets including performance improvement in the prediction on DS11 and DS12. For quantitative performance, Table 6 and Table 7 show the comparison of MSE and R^2, respectively. According to the average value of MSE and R^2, MLP gets inferior performance with the highest error (average MSE = 10.6419) and the lowest compliance between actual data and predicted results (average $R^2 = 0.4143$). This result indicates that conventional neural network architecture cannot provide satisfactory performance in the time-series regression tasks even using non-linear activation function. k-NN achieves better performance than MLP with MSE = 0.4648 and $R^2 = 0.8141$. Moreover, LDA produces slightly better prediction than k-NN (MSE = 0.4179 and $R^2 = 0.8293$). The characteristic of these linear regressors is can predict continuous values very precisely but in other observations also have a high deviation as shown in Fig. 10 a and b. SVR with RBF kernel can produce a lower error (MSE = 0.3687) and higher conformity with actual data ($R^2 = 0.9091$) than the linear regressors. For a time series approach, LSTM has better performance than other conventional algorithms. It gets MSE = 0.1471 and $R^2 = 0.9582$. Finally, DWTLSTM outperforms all of these algorithms with MSE = 0.0515 and $R^2 = 0.9712$. Overall results imply that DWTLSTM produces significantly better performance than other algorithms for regression tasks. It also has better generalization than standard LSTM as shown in Fig. 10e and f. Hence, the results also indicate that DWTLSM produces more stable performances than LSTM on all datasets.

4. Conclusion

In this study, e-nose was used to distinguish four sensory classes and to predict microbial populations in monitoring beef quality. The twelve datasets correspond to various beef cuts were used in this experiment. DWTLSTM was proposed to overcome time-series data from an e-nose that is contaminated with noise. In classification tasks, several machine learning algorithms such as k-NN, LDA, SVR, MLP, and standard LSTM are also used to differentiate four classes of beef in conjunction with e-nose signal. The comparison shows that DWTLSTM gets the highest average accuracy and F-measure. According to the experimental results, conventional algorithms like k-NN, LDA, SVR, MLP susceptible to unable to completely predict four sensory classes of beef in each dataset. On the other side, the neural network architecture specifically for sequential data such as LSTM and DWTLSTM is able to classify four classes of beef. In particular, DWTLSTM has better performance than LSTM in terms of average accuracy and F-measure score. Moreover, it has more stable performance in all datasets. These results imply that DWTLSTM has superior performance than others in classification tasks. Furthermore, the regression tasks are also performed to predict the microbial population in the beef samples. The continuous value of TVC makes it more intricate than the classification task because of the infinite possibilities of class labels. According to the experimental results, DWTLSTM also surpasses k-NN, LDA, SVR, MLP, and standard LSTM. It produces consistent prediction performances on all datasets with lower error as well as higher conformity between prediction results and actual values that are represented by low RMSE and high R^2, respectively. The overall results show that standard LSTM and DWTLSTM have superior performance than other methods both in the classification tasks and regression tasks. The results imply that the time-series approach can produce better performance than conventional methods (k-NN, LDA, SVM/SVR, and MLP). In addition, DWTLSTM has advantages in processing noisy e-nose signals over standard LSTM. Hence, DWTLSTM is also useful to be utilized for other e-nose monitoring applications including smart packaging system, air quality monitoring, production, storage monitoring, and other time series e-nose data processing.

CRediT authorship contribution statement

Dedy Rahman Wijaya: Conceptualization, Methodology, Software, Validation, Formal analysis, Investigation, Resources, Data curation, Writing - original draft, Writing - review & editing, Visualization. **Riyanarto Sarno:** Supervision. **Enny Zulaika:** Resources.

Declaration of Competing Interest

The authors report no declarations of interest.

Acknowledgments

This research was funded by the Indonesian Ministry of Education and Culture, and the Indonesian Ministry of Research and Technology/ National Agency for Research and Innovationunder PTUPT Program

managed by Institut Teknologi Sepuluh Nopember (ITS), and under World Class University (WCU) Program managed by Institut Teknologi Bandung (ITB). This paper is also partially funded by Telkom University. Authors would like to thanks all reviewers who helped improve the quality of this paper.

References

[1] P. Sans, P. Combris, World meat consumption patterns : An overview of the last fifty years (1961–2011), Meat Sci 109 (2015) 106–111.

[2] N. Alexandratos, J. Bruinsma, WORLD AGRICULTURE TOWARDS 2030 / 2050 The 2012 Revision, Rome, 2012.

[3] R.A. Lawrie, The eating quality of meat, 2006, https://doi.org/10.1017/CBO9781107415324.004.

[4] M. Falasconi, I. Concina, E. Gobbi, V. Sberveglieri, A. Pulvirenti, G. Sberveglieri, Electronic Nose for Microbiological Quality Control of Food Products, 2012, 2012, https://doi.org/10.1155/2012/715763.

[5] W. Wojnowski, T. Majchrzak, T. Dymerski, J. Gębicki, J. Namieśnik, Electronic noses: Powerful tools in meat quality assessment, Meat Science. 131 (2017) 119–131, https://doi.org/10.1016/j.meatsci.2017.04.240.

[6] I. Ahmed, H. Lin, L. Zou, Z. Li, A.L. Brody, I. Mabood Qazi, L. Lv, T. Ramesh Pavase, M. Ullah Khan, S. Khan, L. Sun, C. Zhenxing Li, An overview of smart packaging technologies for monitoring safety and quality of meat and meat products, Packaging Technology and Science. 31 (2018) 449–471, https://doi.org/10.1002/pts.2380.

[7] S. Balasubramanian, C.M. Logue, M. Marchello, Spoilage Identification of Beef Using an Electronic Nose System, Transactions of the ASAE. 47 (2004) 1625–1633, https://doi.org/10.13031/2013.17593.

[8] S. Panigrahi, S. Balasubramanian, H. Gu, C.M. Logue, M. Marchello, Design and development of a metal oxide based electronic nose for spoilage classification of beef, Sensors and Actuators, B: Chemical. 119 (2006) 2–14, https://doi.org/10.1016/j.snb.2005.03.120.

[9] N. El Barbri, E. Llobet, N. El Bari, X. Correig, B. Bouchikhi, Electronic Nose Based on Metal Oxide Semiconductor Sensors as an Alternative Technique for the Spoilage Classification of Red Meat, Sensors. 8 (2008) 142–156, https://doi.org/10.3390/s8010142.

[10] S. Balasubramanian, S. Panigrahi, C.M. Logue, H. Gu, M. Marchello, Neural networks-integrated metal oxide-based artificial olfactory system for meat spoilage identification, Journal of Food Engineering. 91 (2009) 91–98, https://doi.org/10.1016/j.jfoodeng.2008.08.008.

[11] Najam ul Hasan, N. Ejaz, W. Ejaz, H.S. Kim, Meat and fish freshness inspection system based on odor sensing, Sensors (Switzerland). 12 (2012) 15542–15557, https://doi.org/10.3390/s121115542.

[12] O.S. Papadopoulou, E.Z. Panagou, F.R. Mohareb, G.J.E. Nychas, Sensory and microbiological quality assessment of beef fillets using a portable electronic nose in tandem with support vector machine analysis, Food Research International. 50 (2013) 241–249, https://doi.org/10.1016/j.foodres.2012.10.020.

[13] F. Mohareb, O. Papadopoulou, E. Panagou, G.-J. Nychas, C. Bessant, Ensemble-based support vector machine classifiers as an efficient tool for quality assessment of beef fillets from electronic nose data, Analytical Methods. 8 (2016) 3711–3721, https://doi.org/10.1039/c6ay00147e.

[14] V.S. Kodogiannis, Application of an Electronic Nose Coupled with Fuzzy-Wavelet Network for the Detection of Meat Spoilage, Food and Bioprocess Technology (2017), https://doi.org/10.1007/s11947-016-1851-6.

[15] D.R. Wijaya, R. Sarno, E. Zulaika, S.I. Sabila, Development of mobile electronic nose for beef quality monitoring, in: 4th Information Systems International Conference 2017, ISICO 2017, Procedia Computer Science, Elsevier B.V., Bali, 2017, pp. 728–735, https://doi.org/10.1016/j.procs.2017.12.211.

[16] V.S. Kodogiannis, A. Alshejari, Neuro-Fuzzy based Identification of Meat Spoilage using an Electronic Nose, in: 2016 IEEE 8th International Conference on Intelligent Systems, IEEE, Sofia, 2016, pp. 710–717, https://doi.org/10.1109/IS.2016.7737406.

[17] S. Omatu, M. Yano, E-nose system by using neural networks, Neurocomputing. 172 (2016) 394–398, https://doi.org/10.1016/j.neucom.2015.03.101.

[18] T.Y. Kim, S.B. Cho, Web traffic anomaly detection using C-LSTM neural networks, Expert Systems with Applications. 106 (2018) 66–76, https://doi.org/10.1016/j.eswa.2018.04.004.

[19] Y. Wu, M. Yuan, S. Dong, L. Lin, Y. Liu, Remaining useful life estimation of engineered systems using vanilla LSTM neural networks, Neurocomputing. 275 (2018) 167–179, https://doi.org/10.1016/j.neucom.2017.05.063.

[20] M. Wielgosz, A. Skoczeń, M. Mertik, Using LSTM recurrent neural networks for monitoring the LHC superconducting magnets, Nuclear Instruments and Methods in Physics Research, Section A: Accelerators, Spectrometers, Detectors and Associated Equipment. 867 (2017) 40–50, https://doi.org/10.1016/j.nima.2017.06.020.

[21] W. Xia, W. Zhu, B. Liao, M. Chen, L. Cai, L. Huang, Novel architecture for long short-term memory used in question classification, Neurocomputing. 299 (2018) 20–31, https://doi.org/10.1016/j.neucom.2018.03.020.

[22] J. Wang, G. Song, A Deep Spatial-Temporal Ensemble Model for Air Quality Prediction, Neurocomputing. 314 (2018) 198–206, https://doi.org/10.1016/j.neucom.2018.06.049.

[23] J. Chung, C. Gulcehre, K. Cho, Empirical Evaluation of Gated Recurrent Neural Networks on Sequence Modeling, NIPS 2014 Deep Learning and Representation Learning Workshop (2014).

[24] R. Jozefowicz, W. Zaremba, I. Sutskever, An Empirical Exploration of Recurrent Network Architectures, in: F. Bach, D. Blei (Eds.), Proceedings of the 32nd International Conference on International Conference on Machine Learning, Journal of Machine Learning Research, Lille, 2015, pp. 1538–1546.

[25] K. Greff, R.K. Srivastava, J. Koutnik, B.R. Steunebrink, J. Schmidhuber, LSTM: A Search Space Odyssey, IEEE Transactions on Neural Networks and Learning Systems. 28 (2017) 2222–2232, https://doi.org/10.1109/TNNLS.2016.2582924.

[26] Y. Tian, K. Zhang, J. Li, X. Lin, B. Yang, LSTM-based Traffic Flow Prediction with Missing Data, Neurocomputing. 0 (2018) 1–9, https://doi.org/10.1016/J.NEUCOM.2018.08.067.

[27] S. Oehmcke, O. Zielinski, O. Kramer, Input quality aware convolutional LSTM networks for virtual marine sensors, Neurocomputing. 275 (2018) 2603–2615, https://doi.org/10.1016/j.neucom.2017.11.027.

[28] W. Bao, J. Yue, Y. Rao, A deep learning framework for financial time series using stacked autoencoders and long- short term memory, Plos One (2017) 1–24, https://doi.org/10.6084/m9.figshare.5028110.

[29] Ö. Yildirim, A novel wavelet sequences based on deep bidirectional LSTM network model for ECG signal classification, Computers in Biology and Medicine. 96 (2018) 189–202, https://doi.org/10.1016/j.compbiomed.2018.03.016.

[30] M. Li, M. Zhang, X. Luo, J. Yang, Combined long short-term memory based network employing wavelet coefficients for MI-EEG recognition, in: 2016 IEEE International Conference on Mechatronics and Automation, IEEE ICMA 2016, IEEE, Harbin, 2016, pp. 1971–1976, https://doi.org/10.1109/ICMA.2016.7558868.

[31] F. Wang, Y. Yu, Z. Zhang, J. Li, Z. Zhen, K. Li, Wavelet Decomposition and Convolutional LSTM Networks Based Improved Deep Learning Model for Solar Irradiance Forecasting, Applied Sciences. 8 (2018) 1286, https://doi.org/10.3390/app8081286.

[32] D.R. Wijaya, R. Sarno, E. Zulaika, Information Quality Ratio as a novel metric for mother wavelet selection, Chemometrics and Intelligent Laboratory Systems. 160 (2016) 59–71, https://doi.org/10.1016/j.chemolab.2016.11.012.

[33] M. Kotarski, J. Smulko, A. Czyewski, S. Melkonyan, Fluctuation-enhanced scent sensing using a single gas sensor, Sensors and Actuators, B: Chemical. 157 (2011) 85–91, https://doi.org/10.1016/j.snb.2011.03.029.

[34] F. Tian, S.X. Yang, K. Dong, Circuit and Noise Analysis of Odorant Gas Sensors in an E-Nose, Sensors. 5 (2005) 85–96, https://doi.org/10.3390/s5010085.

[35] D.R. Wijaya, R. Sarno, E. Zulaika, Sensor Array Optimization for Mobile Electronic Nose: Wavelet Transform and Filter Based Feature Selection Approach, International Review on Computers and Software. 11 (2016) 659–671, https://doi.org/10.15866/irecos.v11i8.9425.

[36] R. Macku, J. Smulko, P. Koktavy, M. Trawka, P. Sedlak, Analytical fluctuation enhanced sensing by resistive gas sensors, Sensors and Actuators, B: Chemical. 213 (2015) 390–396, https://doi.org/10.1016/j.snb.2015.02.114.

[37] C. Wang, L. Yin, L. Zhang, D. Xiang, R. Gao, Metal oxide gas sensors: Sensitivity and influencing factors, Sensors. 10 (2010) 2088–2106, https://doi.org/10.3390/s100302088.

[38] I. Kiselev, V. Sysoev, I. Kaikov, I. Koronczi, R.A.A. Tegin, J. Smanalieva, M. Sommer, C. Ilicali, M. Hauptmannl, On the temporal stability of analyte recognition with an e-nose based on a metal oxide sensor array in practical applications, Sensors (Switzerland). 18 (2018), https://doi.org/10.3390/s18020550.

[39] M. Längkvist, A. Loutfi, Unsupervised feature learning for electronic nose data applied to Bacteria Identification in Blood, NIPS 2011 Workshop on Deep Feature Learning and Unsupervised Learning (2011) 1–7.

[40] L. Pan, S.X. Yang, An electronic nose network system for online monitoring of livestock farm odors, IEEE/ASME Transactions on Mechatronics. 14 (2009) 371–376, https://doi.org/10.1109/TMECH.2009.2012850.

[41] E. Kim, S. Lee, J.H. Kim, C. Kim, Y.T. Byun, H.S. Kim, T. Lee, Pattern recognition for selective odor detection with gas sensor arrays, Sensors (Basel, Switzerland). 12 (2012) 16262–16273, https://doi.org/10.3390/s121216262.

[42] L. Zhang, F. Tian, L. Dang, G. Li, X. Peng, X. Yin, S. Liu, A novel background interferences elimination method in electronic nose using pattern recognition, Sensors and Actuators, A: Physical. 201 (2013) 254–263, https://doi.org/10.1016/j.sna.2013.07.032.

[43] S. Kiani, S. Minaei, M. Ghasemi-Varnamkhasti, A portable electronic nose as an expert system for aroma-based classification of saffron, Chemometrics and Intelligent Laboratory Systems. 156 (2016) 148–156, https://doi.org/10.1016/j.chemolab.2016.05.013.

[44] R. Sarno, D.R. Wijaya, Recent Development in Electronic Nose Data Processing for Beef Quality Assessment, Telkomnika Indonesian Journal of Electrical Engineering. 17 (2019), https://doi.org/10.12928/telkomnika.v16i6.10565.

[45] D.R. Wijaya, F. Afianti, Stability Assessment of Feature Selection Algorithms on Homogeneous Datasets : A Study for Sensor Array Optimization Problem, IEEE Access. 8 (2020) 33944–33953, https://doi.org/10.1109/ACCESS.2020.2974982.

[46] C. Distante, M. Leo, P. Siciliano, K.C. Persaud, On the study of feature extraction methods for an electronic nose, Sensors and Actuators, B: Chemical. 87 (2002) 274–288, https://doi.org/10.1016/S0925-4005(02)00247-2.

[47] C. Distante, M.L, K.C. Persaud, Wavelet Transform for Electronic Nose Signal Analysis, 2011. http://www.intechopen.com/books/discrete-wavelet-transforms-biomedical-applications/wavelet-transform-for-electronic-nose-signal-analysis.

[48] D.R. Wijaya, R. Sarno, E. Zulaika, Noise filtering framework for electronic nose signals: An application for beef quality monitoring, Computers and Electronics in Agriculture. 157 (2019) 305–321, https://doi.org/10.1016/j.compag.2019.01.001.

[49] C. Zanchettin, T.B. Ludermir, Wavelet filter for noise reduction and signal compression in an artificial nose, Applied Soft Computing Journal. 7 (2007) 246–256, https://doi.org/10.1016/j.asoc.2005.06.004.
[50] V.S. Kodogiannis, A. Alshejari, A Fuzzy-Wavelet Neural Network Model for the Detection of Meat Spoilage using an Electronic Nose, in: IEEE World Congress on Computational Intelligence (IEEE WCCI), IEEE, 2016.
[51] D.R. Wijaya, R. Sarno, E. Zulaika, Electronic nose dataset for beef quality monitoring in uncontrolled ambient conditions, Data in Brief. 21 (2018) 2414–2420, https://doi.org/10.1016/J.DIB.2018.11.091.
[52] D.R. Wijaya, R. Sarno, E. Zulaika, Gas Concentration Analysis of Resistive Gas Sensor Array, in: 2016 IEEE International Symposium on Electronics and Smart Devices, IEEE, Bandung, 2016, pp. 337–342, https://doi.org/10.1109/ISESD.2016.7886744.
[53] E. Schaller, J.O. Bosset, F. Escher, Electronic Noses" and Their Application to Food, Lebensmittel-Wissenschaft Und-Technologie. 31 (1998) 305–316, https://doi.org/10.1006/fstl.1998.0376.
[54] A. Graves, Supervised Sequence Labelling with Recurrent Neural Networks, Springer-Verlag Berlin Heidelberg, Berlin, 2012, https://doi.org/10.1007/978-3-642-24797-2.
[55] S. Hochreiter, J. Schmidhuber, Long Short-Term Memory, Neural Computation. 9 (1997) 1735–1780, https://doi.org/10.1162/neco.1997.9.8.1735.
[56] A. Haar, Zur Theorie der orthogonalen Funktionensysteme - Erste Mitteilung, Mathematische Annalen. 69 (1910) 331–371, https://doi.org/10.1007/BF01456326.
[57] R.X. Gao, R. Yan, Wavelets: Theory and Applications for Manufacturing, 2011 editi, Springer, New York; London, 2010.
[58] L. Pasti, B. Walczak, D.L. Massart, P. Reschiglian, Optimization of signal denoising in discrete wavelet transform, Chemometrics and Intelligent Laboratory Systems. 48 (1999) 21–34, https://doi.org/10.1016/S0169-7439(99)00002-7.
[59] C. Saranya, G. Manikandan, A study on normalization techniques for privacy preserving data mining, International Journal of Engineering and Technology. 5 (2013) 2701–2704.
[60] G. Aksu, C.O. Güzeller, M.T. Eser, The Effect of the Normalization Method Used in Different Sample Sizes on the Success of Artificial Neural Network Model, International Journal of Assessment Tools in Education. 6 (2019) 170–192, https://doi.org/10.21449/ijate.479404.
[61] B. KumarSingh, K. Verma, A.S. Thoke, Investigations on Impact of Feature Normalization Techniques on Classifier's Performance in Breast Tumor Classification, International Journal of Computer Applications. 116 (2015) 11–15, https://doi.org/10.5120/20443-2793.
[62] H.K. Patel, The Electronic Nose : Artificial Olfaction Technology, Springer, Ahmedabad, 2014, https://doi.org/10.1007/978-81-322-1548-6_3.
[63] M. Ghasemi-Varnamkhasti, S.S. Mohtasebi, M. Siadat, J. Lozano, H. Ahmadi, S. H. Razavi, A. Dicko, Aging fingerprint characterization of beer using electronic nose, Sensors and Actuators, B: Chemical. 159 (2011) 51–59, https://doi.org/10.1016/j.snb.2011.06.036.
[64] H. Luo, P. Jia, S. Qiao, S. Duan, Enhancing electronic nose performance based on a novel QPSO-RBM technique, Sensors and Actuators, B: Chemical. 259 (2018) 241–249, https://doi.org/10.1016/j.snb.2017.12.026.
[65] D.R. Wijaya, R. Sarno, A.F. Daiva, Electronic Nose for Classifying Beef and Pork using Naïve Bayes, in: International Seminar on Sensor, Instrumentation, Measurement and Metrology (ISSIMM) Surabaya, IEEE, Surabaya, 2017, https://doi.org/10.1109/ISSIMM.2017.8124272.
[66] Hariyanto, R. Sarno, D.R. Wijaya, Detection of diabetes from gas analysis of human breath using e-Nose, in: 2017 11th International Conference on Information & Communication Technology and System (ICTS), IEEE, Surabaya, 2017, pp. 241–246, https://doi.org/10.1109/ICTS.2017.8265677.
[67] S. Jiang, J. Wang, Y. Wang, S. Cheng, A novel framework for analyzing MOS E-nose data based on voting theory: Application to evaluate the internal quality of Chinese pecans, Sensors and Actuators, B: Chemical. 242 (2017) 511–521, https://doi.org/10.1016/j.snb.2016.11.074.
[68] V. Preedy, Electronic Noses and Tongues in Food Science, Elsevier Inc., London, 2016, https://doi.org/10.1016/B978-0-12-800243-8.00002-0.
[69] B.B. Dent, S.L. Forbes, B.H. Stuart, Review of human decomposition processes in soil, Environmental Geology (2003) 576–585, https://doi.org/10.1007/s00254-003-0913-z.
[70] S.L. Forbes, Decomposition chemistry in a burial environment, Soil Analysis in Forensic Taphonomy: Chemical and Biological Effects of Buried Human Remains (2008) 203–223, https://doi.org/10.1201/9781420069921.
[71] CSIRO Food and Nutritional Sciences, Vacuum-packed meat : storage life and spoilage, 2003. http://www.meatupdate.csiro.au/VPmeat-spoilage-storage.pdf.
[72] J.P. Harley, L.M. Prescott, Microbiology 5th ed, Fifth Edit, McGraw-Hill, New York, 2002, https://doi.org/10.1007/s13398-014-0173-7.2.
[73] C.-C. Chang, C.-J. Lin, LIBSVM: A Library for Support Vector Machines, ACM Transactions on Intelligent Systems and Technology 2 (2011) 1–27, https://doi.org/10.1145/1961189.1961199.
[74] Deeplearning4j Development Team, Deeplearning4j: Open-source distributed deep learning for the JVM, Apache Software Foundation License 2.0 (2017). http://deeplearning4j.org.

Dedy Rahman Wijaya was born in Tulungagung, Indonesia, in 1984. He received the bachelor's degree in informatics engineering from STT Telkom Bandung, Indonesia, in 2006, the Master of Engineering degree from the School of Electrical Engineering and Informatics, Institut Teknologi Bandung, in 2010, and the Ph.D. degree in computer science from the Institut Teknologi Sepuluh Nopember, Surabaya, Indonesia, in 2019. He was a Visiting Researcher with the Pulse Lab Jakarta–United Nations Global Pulse, in 2018, where he worked with machine learning and artificial intelligence. He is currently a Lecturer and a Researcher with the School of Applied Science, Telkom University, Bandung. His research interests include cyber-physical systems, intelligent systems, information, signal processing, and machine learning including their applications.

Riyanarto Sarno since 2003 is Professor of Software Engineering at ITS Surabaya, born in Surabaya in 1959. Education from elementary to high school is completed in Surabaya. Graduated with a Bachelor of Electrical Engineering at ITB in 1983 and a Bachelor of Economics in UNPAD in 1985. He completed his Masters (MSc) and Doctor of Science (PhD) in Computer Science at the University of New Brunswick Canada in 1988 and 1992. At ITS, he served as Chair of the Center for Computer Research and Information Systems, Chair of the Community Service Institute, Head of the Software Engineering Laboratory and Dean of the Faculty of Information Technology. In order to establish international relations, he was appointed as Adjunct Professor at the University of New Brunswick Canada from 2004 to 2008. Prof. Riyanarto is also active in various national professional organizations such as PII, ISEI, EKONID and CALINDO. International professional organizations that are followed include the Institute of Electrical and Electronics Engineers (IEEE), the Association for Computing Machinery (ACM) and the Information Systems Audit and Control Association (ISACA).

Enny Zulaika received M.P in Biology from the Brawijaya University in 1997 and received Ph.D. degree in Biology from Airlangga University in 2013. Her research interests are bioremediation and biodegradation.